Chapter 6

Cluster Predissociation Spectroscopy of Protonated Anthracene

6.1 Introduction

As determined in Chapter 5, protonated PAHs are very photostable – a fact that makes recording their direct dissociation spectra with nanosecond lasers quite difficult. To enable single photon experiments to be conducted, the spectra of van der Waals clusters of protonated PAHs with volatile atoms or molecules may be recorded. Since van der Waals interactions are much weaker than chemical bonds, even the vibrational excitation of intramolecular bonds in the components can lead to dissociation. Recording the photodissociation of the cluster gives the predissociation spectrum of the chromophore molecule or ion in the cluster. The spectral lines of the cluster are shifted from the gas phase values of the chromophore due to its interaction with the cluster partner. For clusters with rare gases, the shift is usually within 100 cm^{-1}.

The cluster photodissociation method has been successfully used in the past to record the vibrational [3, 96, 150–154] and electronic [71–74] spectra of clusters of protonated benzene and PAH cations with rare gases. Here it is used to record the visible spectrum of protonated

anthracene.

6.2 Experiment

Ideally, for optimum cluster production, the partner gas should be mixed with protonated PAHs in the discharge under high pressure and then expanded into vacuum. In most experiments, the number of molecules for this gas significantly exceeds the number of PAH molecules. The single-valve discharge source (Chapter 4, 4.2) that has been used to protonate PAHs has an inconvenient property in this regard. Whenever a third gas is added to the hydrogen:PAH mixture, it changes the discharge charge transfer characteristics because the cluster partner competes with PAH molecules for protonation. As a result, the PAH protonation efficiency is decreased. For example, no protonation was observed for anthracene when the discharge was run with 1% of argon added to mixture.

To avoid this problem, the third gas can be mixed into the discharge flow after the protonation has already happened. This may be done either in a crossed molecular beam setup, or as the ions expand into vacuum. The latter method also helps to cool the clusters and therefore, was selected here. In particular, the clusters of protonated anthracene with water were made in the two-valve discharge source described in Chapter 4 (4.3) with the second pulsed valve used to deliver the cluster partner into the discharge through two symmetric channels in the last electrode. When the pressure and delay times were adjusted properly, the third gas was picked up by the discharge stream and carried into vacuum without entering the discharge.

Argon, krypton and xenon were first tested as the cluster partner, but they did not produce any clusters with protonated anthracene. Apparently, the discharge was too hot and the pressure at the mixing point was not high enough to provide the cooling needed

for cluster formation. A molecule that would create a stronger bound cluster is needed.

Water and ammonia are well known for their ability to cluster with other molecules and were therefore tested as well. One important consideration here is the effect of the cluster partner on the protonated PAHs. The proton affinities of PAHs are in 190 – 210 kcal/mol range and that for H_2O and NH_3 is 165 kcal/mol and 204 kcal/mol, respectively [113]. Since the proton affinity of water is lower than that for PAHs, it will not significantly affect the protonation level of ground state PAH molecules. Ammonia, on the other hand, may attract the proton, thus making a cluster of a neutral PAH and protonated ammonia instead of protonated PAH and ammonia. For this reason, ammonia was discarded.

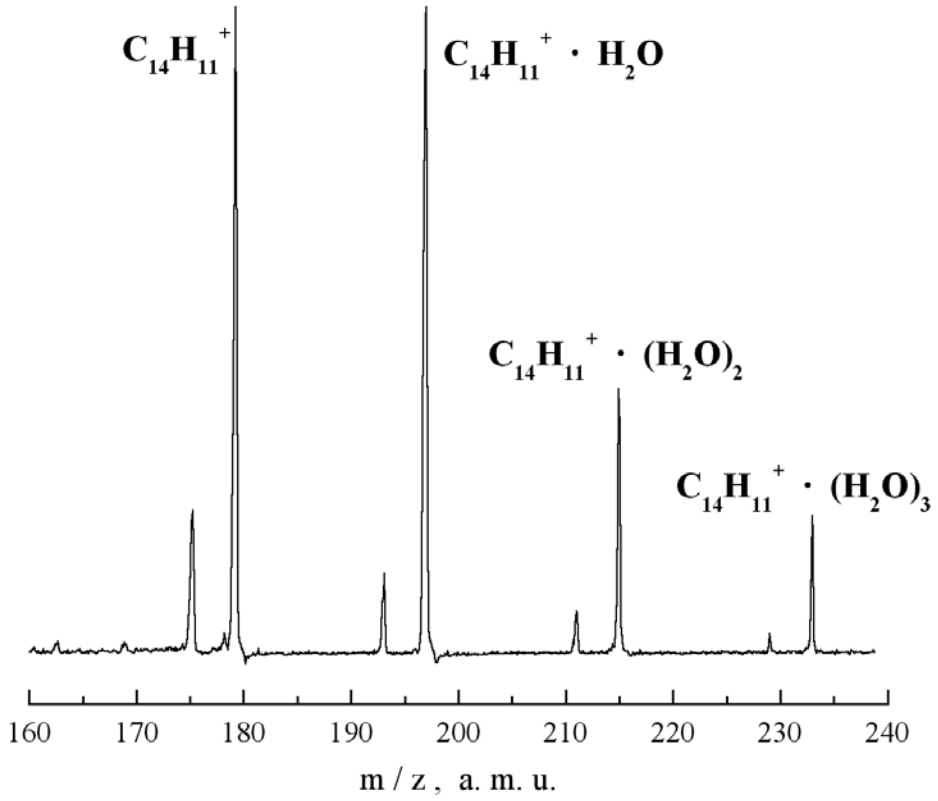

Figure 6.1: A mass spectrum of the two-nozzle source of protonated anthracene–water clusters.

Hydrogen was flowed over the surface of distilled water and used as a carrier gas to deliver H_2O molecules to the discharge. This method was preferred over hydrogen bubbling through water since it assured more stable pressure for the H_2O/H_2 mixture. With this setup, the water mixing ratio and the total pressure in the mixing region was high enough to allow clustering. Indeed, water was found to cluster with protonated anthracene very efficiently. Clusters with up to three water molecules were observed (Figure 6.1). Spectroscopy could be performed with any of these clusters, but $C_{14}H_{11}^+ \cdot H_2O$ was selected as it possessed the strongest and most stable signal.

The experiments were performed in the same way as that outlined for the photodissociation of protonated PAHs in Chapter 5, with the OPO with mixed BBO Type I and II rotated prism cavity (Chapter 4, 4.6) used as the laser source.

6.3 Results and Discussion

6.3.1 Cluster Geometry

The geometry of PAH $\cdot$ H_2O clusters is determined by the balance of the electrostatic interaction and repulsive forces between the cluster partners. For example, in $C_6H_6 \cdot H_2O$

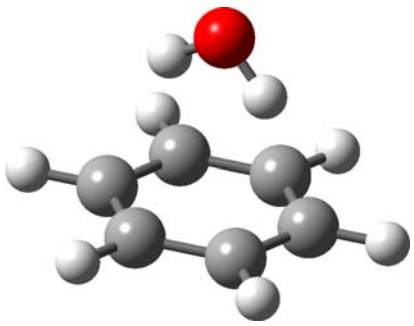

Figure 6.2: The benzene–water ($C_6H_6 \cdot H_2O$) dimer geometry.

(Figure 6.2), the water molecule binds with its hydrogens pointed toward the π aromatic system of benzene [155], thanks to the electrostatic interaction of the water molecule dipole moment with the quadrupole moment of the benzene molecule.

The picture is different in the case of protonated PAHs since they are a positively charged species. To zeroth order, the electrostatic interaction is dominated by charge-dipole forces. As a result, water prefers to bind via the oxygen side and can no longer bind to the aromatic system of protonated PAH due to the repulsion between the aromatic π system electrons and the oxygen lone pairs. Hence, water binds in the PAH plane. To be more precise, it will bind to the site with the largest positive charge: the CH_2 site hydrogens. The cluster geometry for isomer 1 of protonated anthracene was optimized at a low level of theory and is shown in Figure 6.3. The geometry is similar to that of the protonated benzene–water cluster [156], although for $C_6H_7^+ \cdot H_2O$, the isomer of the cluster with the bridged stricture was estimated to be more stable.

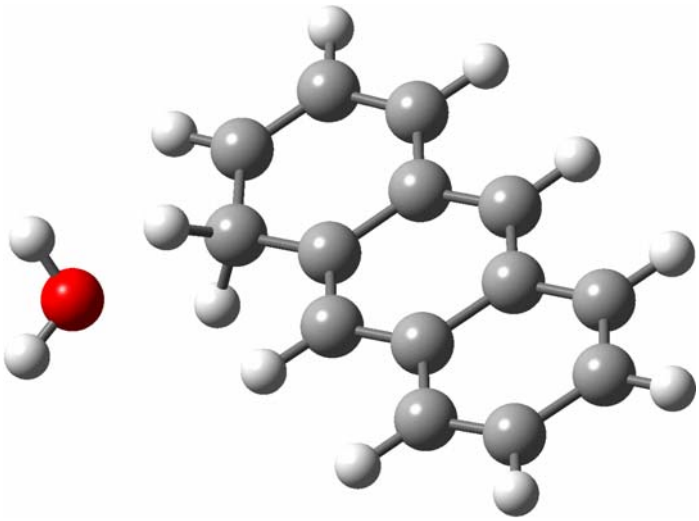

Figure 6.3: Protonated anthracene–water (1–$C_{14}H_{11}^+ \cdot H_2O$) cluster geometry.

It is not known whether successive water molecules bind to the PAH protonation site or to other H_2O molecules in the cluster. This question, however, is not considered further as no results were acquired for $C_{14}H_{11}^+ \cdot (H_2O)_n$, $n \geq 2$.

6.3.2 Measured Spectrum

The photodissociation spectrum of the $C_{14}H_{11}^+ \cdot H_2O$ cluster was recorded in the 422 – 540 nm range with a resolution of 0.1 nm. Longer wavelengths were not scanned because no excited states for protonated anthracene were predicted to lie at such low energies. The predicted dissociation products are protonated anthracene and water, but this could not be verified experimentally. The neutral product (presumably H_2O) signal was normalized by the value of the cluster signal without the laser, and by the laser pulse energy. The resulting absorption spectrum is shown as the upper trace in Figure 6.4.

At longer wavelengths, there is no measurable absorption. As the wavelength is decreased, the cluster begins to absorb with a threshold wavelength of ∼490 nm. The absorption continually increases toward the blue and is never saturated. The maximum cluster dissociation occurred at 435 nm, where the dissociation efficiency reached 50% due to higher OPO pulse energies.

At first glance, the spectrum appears nearly exponential. A more careful inspection reveals two noticeable bumps that we assign to the excited electronic states of protonated anthracene isomers. The spectrum can be fit nicely by an exponential (grey curve) and two Gaussian or Lorentzian (blue and green curves) functions, resulting in the red curve. The lower trace in Figure 6.4 is the spectrum at the top with the exponential dependence removed for better contrast in the remaining features. Here, the red curve displays the fit of the two Lorentzians alone (fits with Gaussians are quite similar).

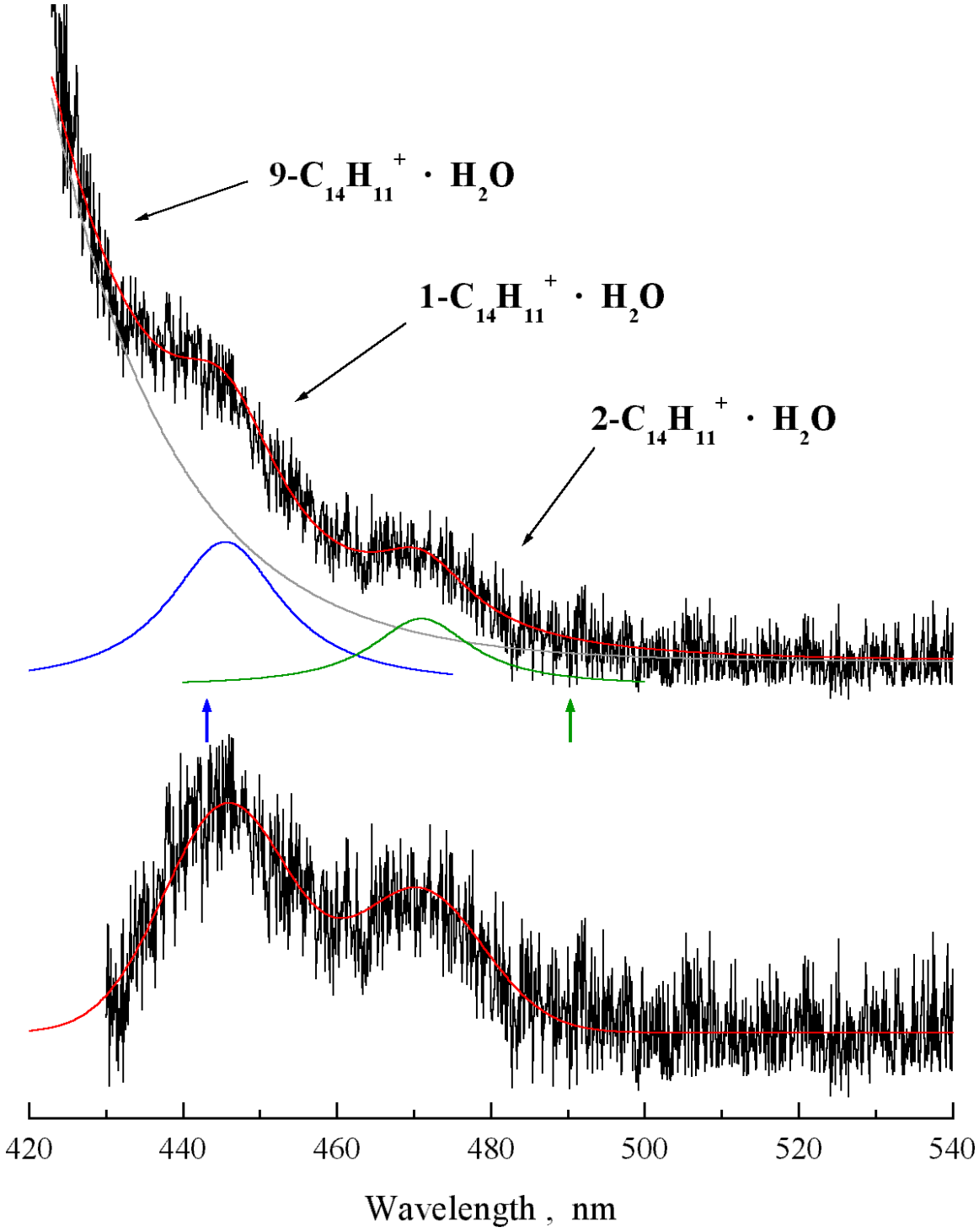

Figure 6.4: Protonated anthracene–water ($C_{14}H_{11}^{+} \cdot H_2O$) cluster photodissociation spectrum. Top: The recorded spectrum and exponential+Lorentzian fit. Bottom: Data with the exponential rise to short wavelengths removed.

We base our assignment of the observed bands to the $S_1 \leftarrow S_0$ transition for protonated anthracene based on the excited state calculations presented in Chapter 3. The longer wavelength band corresponds to isomer 2 of protonated anthracene, while the shorter wavelength band corresponds to isomer 1. The overall exponential increase at short wavelengths is most likely due to the most stable isomer, isomer 9, but a final assignment of this blue increase may only be accomplished when the spectrum down to ∼350 nm is recorded.

Isomer 9 is more stable than the other two isomers by ∼10 kcal/mol and isomer 1 is more stable than isomer 2 by 3 kcal/mol. If the clusters are in thermodynamic equilibrium, the majority of them will be in the form of isomer 9. Similarly, the oscillator strength for isomer 9 is twice as large as for isomer 1, which in turn, has a larger oscillator strength than isomer 2 (Table A.37 in Appendix A). The combined effects of the isomer population distribution and the inherent strengths of the bands may explain the steep rise in absorption at short wavelengths.

6.3.3 Band Positions and Widths

In the fit to the measured spectrum, the two gaussian curves have their maxima at 445.8 nm and 470.7 nm, with full width at half maxima (FWHM) of 19.6 nm. For Lorentzian fits to the data, band positions of 445.5 and 471.0 nm are derived with FWHM of 17.2 and 16.0 nm, respectively. In either case, the band origins (that is, the wavelength of the feature maximum) are about 445.6 nm for isomer 1 and 471 for isomer 2. The predicted transition wavelengths (443.1 nm and 490.4 nm) are shown in Figure 6.4 as vertical arrows. The predicted transition wavelength for isomer 1 is remarkably close to the band origin in the measured spectrum (443.1 nm *vs.* 445.6 nm), while for isomer 2 the experimental value is shifted to the blue by ∼19 nm from that predicted.

At the available signal-to-noise ratio, no internal structure is seen in the bands. The spectra are either vibrationally or lifetime broadened. The vibrational broadening of the excited state leads to band blue shift, while the vibrational broadening of the ground state and the lifetime broadening are expected to work in both directions from the band origin.

6.3.4 Comparison with Spectra of Other Clusters

The measured $C_{14}H_{11}^{+} \cdot H_2O$ cluster spectrum should be compared to the spectra of similar clusters in order to draw any conclusions about the cluster properties and especially about the spectrum of bare protonated anthracene. The dissociation spectrum for the naphthalene cation–argon cluster [71, 73] is red-shifted from the gas phase spectrum of the naphthalene cation [62] by 2 nm (50 cm^{-1}), but has similar widths (25 – 30 cm^{-1} FWHM) of the vibronic features therein. For the phenanthrene–argon cluster [72,73], the red shift is 13 cm^{-1}. REMPI spectral lines for the anthracene–argon cluster [69] are also very narrow (10 cm^{-1} FWHM) and the red shift is 47 cm^{-1}. However, these shifts are for clusters with argon, whose spectra do not have as large a red shift as those with polar molecules. For clusters of anthracene with water [157] and methanol [158], the band widths increase slightly compared to those with Ar but are no more than 30 – 40 cm^{-1}, and the red shifts remain tolerably small at 100 – 150 cm^{-1}.

Based on these data, one would expect the absorption bands for the protonated anthracene–water cluster to be no more than 50 cm^{-1} wide, versus the measured value of 1100 cm^{-1}. The red shift in the protonated anthracene gas phase spectrum would be about 100 – 200 cm^{-1} (4 nm) if it behaved similarly to PAHs and PAH cations. The comparison of the calculated $S_1 \leftarrow S_0$ transition wavelength (as in Chapter 3) for isomer 1 of protonated anthracene and its cluster with water gives a similar shift value. Using these shifts and the measured

band origins, the photodissociation spectrum for the $C_{14}H_{11}^{+} \cdot H_2O$ cluster should look similar to that shown in Figure 6.5. Clearly, this is not the case. Thus, absorption bands as measured experimentally must be broadened by either a property intrinsic to protonated anthracene or created by the cluster environment.

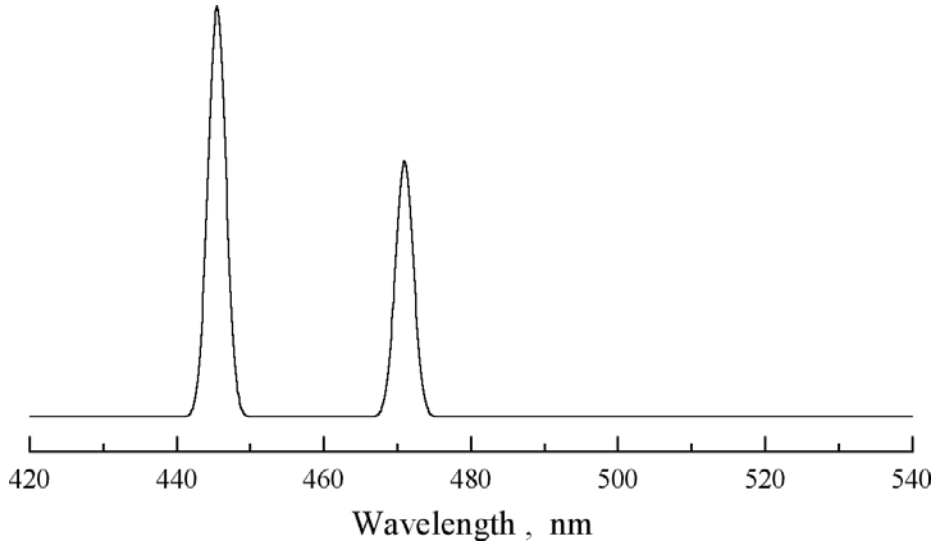

Figure 6.5: The expected protonated anthracene–water cluster photodissociation spectrum from comparisons with PAH and PAH^{+} clusters.

6.3.5 Effect of Proton Mobility on the Spectral Width

To answer the important question, "What causes the widths of measured bands to be as high as 1100 cm^{-1} (FWHM)?", several scenarios must be considered. Is it due to some experimental procedure, or is it due to a property of the cluster or of protonated anthracene itself?

As was found in Chapter 2, protonated aromatics have one thing in common that neutral PAHs and their cations do not: an ability to isomerize by proton hopping from one carbon atom to another. This dramatically increases the density of vibrational states for the highly

excited protonated PAHs, increase that is largely due to the contribution of all isomers since they are coupled to each other. No such coupling exists for neutral PAHs and their cations, and although they have nearly the same number of atoms (and hence the number of vibrational modes) as protonated PAHs, only one isomer is possible.

When a protonated PAH absorbs a visible or UV photon and becomes excited electronically, it can non-radiatively transfer to the ground electronic potential energy surface via internal conversion. The density of vibrational states on the ground state at an excitation of 10,000 – 25,000 cm^{-1} is the crucial consideration. Higher densities of vibrational states lead to faster internal conversion, shorter excited state lifetimes and broader spectral features. This lifetime broadening mechanism will not depend on whether the protonated PAH exists freely or as a member of a cluster, and explain why the protonated benzene photodissociation spectrum [90] is as broad as the protonated anthracene–water bands observed here.

6.3.6 Other Factors

If protonated anthracene in a cluster retains vibrational excitation, additional spectral broadening of the predissociation spectrum can result. Since protonated anthracene was made in a discharge, it is expected to be vibrationally warm, thanks to the high electron temperature of such environments. This is the likely explanation for why the attempts to generate protonated PAH clusters with rare gases were unsuccessful. On the other hand, the clusters cannot be too hot because clusters with up to three water molecules were produced. Based on this observation, one would expect the vibrational temperature of the clusters be somewhere in the range of 50 – 150 K. At these temperatures, intermolecular and the very lowest intramolecular modes could be populated, but it is unlikely they could cause the

level of broadening observed or create a spectral profile that is as smooth as that measured experimentally.

Another thing that may lead to spectral broadening is C–H bond softening at the protonation site through interactions with the water molecule. For the protonated benzene–water dimer, for example, the energy difference between the two protonation sites (one on benzene, the other on water) was calculated to be only 2.6 kcal/mol [156] with a barrier to proton transfer of only 2.5 kcal/mol, despite the fact that the proton affinity of benzene is 14.3 kcal/mol larger than in water. The effect should be not as noticeable in the protonated anthracene–water cluster since the proton affinity of anthracene is higher than for benzene by another 20 – 30 kcal/mol, depending on the protonated isomer (1, 2, or 9).

6.3.7 Comparison with the DIBs

There is a strong diffuse interstellar band at 4430 Å (FWHM = 1.15 nm) which is very close to the expected band origin of the transition for isomer 2 of protonated anthracene (Chapter 3, Figure 3.4). There are also four broad diffuse interstellar bands in the 470 – 500 nm region, one of which (λ_{max} = 476.2 nm, FWHM = 2.36 nm) red-shifted by ∼6 – 10 nm from the expected band origin of the isomer 2 transition. This is a rather large discrepancy for a good match, but given the uncertainties in the cluster spectrum, the coincidence is worth considering further if additional experimental data are generated. Little can be said at present about isomer 9. Further, even the broadest currently known DIB features are one order of magnitude narrower than the measured bands. Thus, it is most likely that protonated anthracene is not a DIB carrier. Such broad electronic transitions do make protonated PAHs excellent 'harvesters' of interstellar visible and UV photons, however, and this combined with the high photostability makes them excellent candidates for UIR

emitters.

If other protonated PAHs have electronic absorption spectra with bands that are similarly broadened, they are equally unlikely to be DIB carriers. This depends largely on the spectral broadening nature. If the proton mobility is a major factor to that, then the isomerization within one PAH ring is a larger contributor then the isomerization across the ring fusion, because such process has a higher barrier. This may lead to narrower absorption band widths in species like coronene. If the vibrational temperatures of protonated PAHs in the ISM are lower than those in laboratory experiments, interstellar absorption bands may be even narrower. The cumulative effect of these factors may bring the expected interstellar band widths close to those for wide DIBs.

6.4 Summary

The visible photodissociation spectrum of the protonated anthracene–water ($C_{14}H_{11}^{+} \cdot H_2O$) cluster was recorded using our modified BBO OPO type I and type II cavity. The two absorption bands observed were assigned to isomers 1 and 2 of protonated anthracene. The origin of one of these bands was very close to the predicted value, but the observed absorption bands were very broad: FWHM were close to $\simeq$ 20 nm or 1100 cm^{-1}. The smooth nature of the bands suggests that a substantial component of the broadening is most likely due to the increase in the density of vibrational states resulting from the proton mobility in protonated anthracene. Internal vibrational excitation of the anthracene or of the cluster intermolecular modes may contribute as well, as may proton transfer interactions with the water molecule.

The measured absorption bands are 10 times wider than even the broadest diffuse interstellar bands. While there is a DIB next to the band origin for isomer 1 of protonated

anthracene, no such close coincidence exists for isomer 2. Protonated anthracene is therefore unlikely to be a DIB carrier. If all protonated PAHs share the dynamical properties of $C_{14}H_{11}^{+}$ inferred from the predissociation spectrum, there role as DIB carriers is suspect as well. The excellent photostability of these species, along with their vibrational band positions, however, means that they would be very efficient sources of UIR emission.